Received: 24 March 2021 | Revised: 23 June 2021 | Accepted: 6 July 2021

DOI: 10.1002/psp4.12692

ARTICLE

Population pharmacokinetic analysis of ulotaront in subjects with schizophrenia

Gerald R. Galluppi[1] | **Daniel G. Polhamus**[2] | **Jeannine M. Fisher**[2] | **Seth C. Hopkins**[1] | **Kenneth S. Koblan**[1]

[1]Sunovion Pharmaceuticals Inc, Marlborough, Massachusetts, USA

[2]Metrum Research Group, Tariffville, Connecticut, USA

Correspondence
Gerald R. Galluppi, Clinical Pharmacology, Sunovion Pharmaceuticals, 84 Waterford Dr., Marlborough, MA 01752, USA.
Email: gerald.galluppi@sunovion.com

Funding information
This study was funded by Sunovion Pharmaceuticals, Inc. Dr. Edward Schweizer of Paladin Consulting Group provide editorial assistance in the preparation of the manuscript that was funded by Sunovion Pharmaceuticals, Inc.

Abstract

Ulotaront (SEP-363856) is a trace amine–associated receptor 1 agonist with 5-HT_{1A} agonist activity in phase III development for the treatment of schizophrenia. The efficacy of ulotaront is not mediated by blockade of D_2 or 5-HT_{2A} receptors. The aim of this study was to evaluate the population pharmacokinetics (PopPKs) of ulotaront in adult subjects using pooled data from seven phase I studies, one phase II acute study, and one 6-month extension study. Single and multiple (up to 7 days) oral doses (5–150 mg/day) were studied in both healthy adult subjects (with intensive serial plasma sampling) and adult patients with schizophrenia (some with intensive and some with sparse plasma sampling). Ulotaront was well-absorbed and exhibited dose-proportionality in doses ranging from 10 to 100 mg, in mean maximum concentration, area under the concentration-time curve, and minimum concentration. Moderate interindividual variability was observed in concentration-time profiles. The estimated median time to maximal concentration was 2.8 h and the median effective half-life was 7 h, corresponding to an exposure accumulation ratio of 1.10 at steady-state with daily dosing. There was no indication of time-dependent changes in PKs after up to 12 weeks of daily dose administration. No clinically meaningful effects on ulotaront PK parameters were observed based on race, age, sex, formulation (capsule or tablet), or clinical status (healthy volunteer vs. patient with schizophrenia); body weight was the only meaningful covariate.

Study Highlights

WHAT IS THE CURRENT KNOWLEDGE ON THE TOPIC?

This is the first published pharmacokinetic (PK) analysis of ulotaront, a novel non-D2 treatment for schizophrenia that acts via trace amine–associated receptor 1 and 5-HT1A agonist activity. Ulotaront has received breakthrough therapy designation by the US Food and Drug Administration.

WHAT QUESTION DID THIS STUDY ADDRESS?

The primary objective of the current study was to characterize the population (Pop)PKs of ulotaront using plasma concentration-time data from single and multiple dose administrations in adult subjects, and to characterize potential covariates of the PKs of ulotaront, including clinical status, race, sex, age, and body weight.

WHAT DOES THIS STUDY ADD TO OUR KNOWLEDGE?

The study provides the first PK data on ulotaront, demonstrating that it is well-absorbed, exhibits dose-proportionality, and summarizes key PK parameters (e.g., time to maximal concentration, maximum concentration, and area under the concentration-time curve).

HOW MIGHT THIS CHANGE DRUG DISCOVERY, DEVELOPMENT, AND/OR THERAPEUTICS?

The results of the study have provided guidance on dosing schedules to be used during the currently ongoing clinical development program for ulotaront.

INTRODUCTION

Since the introduction of chlorpromazine 65 years ago, the treatment of schizophrenia has relied exclusively on drugs that act via antagonist or partial agonist effects at postsynaptic dopamine D_2 receptors. This includes second-generation ("atypical") antipsychotic agents, which have additional antagonist activity at serotonin 5-HT_{2A} receptors resulting in a safety profile characterized by a reduction in extrapyramidal symptoms but an increased risk of weight gain and metabolic parameters with the long-term potential for cardiovascular consequences.[1–5] Efficacy is comparable for both first- and second-generation D_2 receptor-binding antipsychotics, with limited benefit noted in treating negative symptoms (e.g., blunted affect and anhedonia) and cognitive impairment, two areas of high unmet need in the treatment of schizophrenia.[2,6,7]Trace amine–associated receptor 1 (TAAR1) has been identified as a novel therapeutic target for the treatment of schizophrenia and other psychiatric disorders. TAAR1 is a G-protein–coupled receptor that modulates dopaminergic, serotonergic, and glutamatergic signaling and is expressed throughout the central nervous system (CNS), including the ventral tegmental area, the dorsal raphe nucleus, the amygdala, the hypothalamus, prefrontal cortex, and the subiculum.[8-13] TAAR1 knockout mice exhibit increased striatal D2 receptor expression and dopamine supersensitivity that resembles aspects of positive symptoms of schizophrenia, whereas agonist activity at TAAR1 receptors has been shown to decrease dopamine neuron firing and release.[8,14,15] Based on these findings, TAAR1 supersensitivity holds promise as a therapeutic target for a range of neuropsychiatric disorders that involve dysregulated monoaminergic signaling, such as schizophrenia, addiction, depression, attention-deficit/hyperactivity disorder (ADHD), Parkinson's disease, and obsessive-compulsive disorder (OCD).[10–13]

Ulotaront (SEP-363856) is a TAAR1 agonist with 5-HT_{1A} agonist activity that is currently in phase III clinical development for the treatment of schizophrenia.[16] Ulotaront is a highly soluble, highly permeable compound (Biopharmaceutics Classification System [BCS] Class I drug product) that is well absorbed (>95%) following oral administration. Ulotaront is cleared via a combination of metabolism (85%) and excretion (15%) of the parent molecule. Unlike atypical antipsychotic agents, ulotaront does not mediate its effects via blockade of D_2 or 5-HT_{2A} receptors. Ulotaront has demonstrated efficacy in mouse models assessing endophenotypes of schizophrenia, including phencyclidine (PCP)-induced hyperactivity, prepulse inhibition, and PCP-induced deficits in social interaction.[16] Suppression of rapid eye movement sleep has also been reported in both rats and humans.[16,17] In addition, ulotaront attenuated the ketamine-induced increase in striatal dopamine synthesis capacity without producing an effect in naïve mice, suggesting that it may modulate presynaptic dopamine dysfunction observed in patients with schizophrenia.[18] In a randomized, double-blind, placebo-controlled clinical trial in patients with an acute exacerbation of schizophrenia, treatment with ulotaront (50 or 75 mg/day) demonstrated significant reduction in symptoms of schizophrenia.[19] Treatment with ulotaront was not associated with extrapyramidal symptoms or elevations in prolactin that are common in antipsychotic agents that act via D2-receptor blockade.

The primary objective of the current study was to characterize the population (Pop)PKs of ulotaront using plasma concentration-time data from single and multiple dose administrations in adult subjects and to characterize potential covariates of ulotaront PK, including clinical status (healthy volunteer vs. patient with schizophrenia),

race (Asians vs. non-Asians), sex, age (18–55 years), formulation (capsule or tablet), and body weight.[20,21]

METHODS

All clinical studies were reviewed and approved by a central institutional review board and were conducted in accordance with Good Clinical Practice and the Declaration of Helsinki. The benefits and risks of study participation were reviewed with each participant, and written informed consent was obtained from all participants before any study procedures were performed.

Subjects

Studies enrolled adults aged 18 to 55 years. For the studies enrolling patients with schizophrenia, all subjects needed to meet the Diagnostic and Statistical Manual of Mental Disorders Fourth Edition; Text Revision (DSM-IV-TR)[22] or DSM-5[23] criteria for a primary diagnosis of schizophrenia. Additional entry criteria included a Clinical Global Impression-Severity of Illness (CGI-S)[24] score less than or equal to 4 and a Positive and Negative Syndrome Scale (PANSS)[25] total score less than or equal to 80.

In the eight studies, ulotaront doses from 5 mg through 150 mg q.d. were evaluated with a variety of study designs that collected both intensive and sparse plasma ulotaront concentration-time samples. Two different assays for ulotaront were used across the trials leading to a lower limit of quantification (LLQ) of 0.02 ng/ml in studies SEP361-101, SEP361-102, SEP361-103, SEP361-105, SEP361-106, and SEP361-111, whereas the two Japanese studies (DA801002 and DA801004) as well as the phase II studies had a higher LLQ of 0.25 ng/ml.

The populations, study design, doses administered, expected sample size, and degree of PK sampling for each of these studies are summarized in Table S1.

Population pharmacokinetic analysis dataset

PK data from eight separate studies were pooled for the current analyses. Seven of the studies were phase I and one study was phase II with an open-label extension study. All phase I studies used a capsule form of ulotaront and included a PK bioequivalence confirmation (SEP361-111) of capsule and tablet forms. The phase II study and open-label extension was performed with ulotaront tablets. After removing samples taken from subjects on placebo, the analysis data set consisted of 4149 plasma concentration observations from 404 subjects who received at least one dose of ulotaront. Across all studies, 9.4% of the samples taken after receiving active drug were below the lower limit of quantification (BLQ); most of these occurred in the intensive sampling studies at later time points (i.e., past 48 h after last dose). Inclusion of the BLQ observations was not considered in the model-fitting steps of the analysis, but the missingness patterns are consistent with the rapid clearance exhibited by this compound. Composite plots of the concentration versus time data for each study and treatment, on a semi-log y-axis scale, are provided in the online Supplemental section (Figures S1–S11).

The study population consisted of 99 healthy volunteers and 305 patients with schizophrenia, 286 men and 118 women with ages ranging from 18 to 55 years (mean [SD] = 33.3 [8.7]) and weights ranging from 45.2 to 135.9 kg (mean [SD] = 77.7 [15.7]). Of the 404 PK-evaluable subjects, 53.7% were White, 31.4% Black, 10.9% Asian, and 3.9% other/mixed race. Of note, over 80% of Asian subjects in the analysis set were from the Japanese studies; as such, subjects referenced as Asian in Asian / non-Asian comparisons should be considered primarily Japanese. As expected, the Japanese studies (DA801004 and DA801002) tended to be lower in body weight. In the United States and global studies, the racial distribution was mostly White and Black (African American), whereas all subjects in the Japanese studies were of Asian descent.

Model development

Ulotaront concentration in plasma relative to the time of administered dosing was a primary analysis variable. Population PK analyses for repeated-measures end points were conducted via nonlinear mixed effects modeling with a qualified installation of the nonlinear mixed effects modeling (NONMEM) software, version 7.4.3 (ICON Development Solutions, Hanover, MD). Initial modeling was conducted using a one-compartment model with first-order absorption parameterized in terms of apparent clearance after oral dosing (CL/F), apparent volume of distribution after oral dosing (V/F), and absorption rate constant (k_a), with appropriate random effect distributions. The model was extended to a two-compartment model, adding intercompartmental clearance (Q/F) and peripheral volume (Vp/F). Other absorption models, such as addition of absorption lag and zero-first-order absorption, were evaluated with the final structural model chosen per goodness-fit-criteria (Akaike information criterion [AIC]) as well as inspection of typical visual diagnostics for nonlinear mixed effects models. To assess the effect of covariates,[26] a full model was constructed including

several factors identified of specific clinical interest: patient status (healthy volunteer vs. patient with schizophrenia), sex, weight (kg), age (years), and ethnicity (Asian/non-Asian). No dimensionality reduction was performed (i.e., the full model approach was used), a simplification of the global model approach described by Burnham and Anderson[27] to allow for inference on the covariates of clinical interest. Population parameters, including fixed effects parameters (covariate coefficients and structural model parameters), and random effects parameters were estimated. An exploratory assessment of any remaining trends was conducted by graphical inspection of all covariate effects, Bayes estimates of individual random effects, and/or weighted residuals. The full model and parameter estimates were investigated with visual predictive checks (VPCs) and posterior predictive checks, details are provided in the online Supplementary section.

Model-based inference

The full model was applied to several inferential tasks to inform decision making in product development, details for each are given in the online Supplementary section. Typical concentration time curves for patients with schizophrenia at doses of 25, 50, 75, 100, 125, and 150 mg once daily (q.d.) dosing were generated for illustrative purposes of PKs under repeated dosing. Covariate effects were also assessed via simulation to illustrate their extent of influence on steady-state exposure metrics. Simulation was also used to characterize other pertinent PK characteristics of the compound (e.g., time to maximum concentration (T_{max}), effective terminal half-life [$t_{1/2,eff}$] and accumulation ratio.[28]

Dose proportionality was examined using two different graphical approaches focusing on the full PopPK model results. The first approach considered the distribution of the individual PK parameter random effects (i.e., η_i) across the maximal dose received in the trial setting for all phase I patients in the analysis population. As η_i represents the difference from the population mean per PK parameter, trends in the dose-η relationship indicate violation of dose proportionality. The second approach aimed to illustrate dose-proportionality of area under the concentration-time curve for a dosing interval (AUC_{0-24}), and maximum concentration (C_{max}) using observed dosing and model-predicted concentration (i.e., without residual variability in PKs affecting the AUC and C_{max} calculations). Each patient's longitudinal PK profile was simulated conditional on their observed dosing and estimated PopPK parameters. PK observations were simulated at 15-minute intervals, and then AUC_{0-24} and C_{max} for the doses on intensive sampling days for each patient were calculated. For each dose, the geometric mean of the simulated PopPK metrics was calculated along with its 95% confidence interval (CI) and then plotted against the administered doses. Doses at which the 95% CI did not include the linear fit through the dose-geometric-mean relationship were considered doses in violation of proportionality.

Applications of modeling and simulation

Simulation of phase III clinical trial and the need for +2 h time point to estimate volume of distribution

A planned phase III study aims to include a cohort ($n = 90$) of adolescent patients with schizophrenia (13 to 17 years) to characterize ulotaront in younger populations than those studied in the initial development program. To evaluate the informativeness of the planned PK sampling scheme, simulations were performed to determine whether the study was sufficiently powered to target a 95% CI within 60% and 140% of the geometric mean estimates of Cl and Vc (i.e., with at least 80% power).[29] Patient PK was to be assessed predose on the night of the first dose, and ~ 10–15 h postdose (AM PK sampling) on days 8, 15, and 43. A simulation approach was used to assess the power of this sampling scheme as well as the potential improvement by adding a single sample after the first dose. The NHANES database[30] was leveraged to sample weights at adolescent (13–17) ages and then adolescent PK was simulated from the full PK model at the planned sampling times and at additional sample times after the first dose (i.e., 1 to 12 h). Each simulated trial was estimated using a two-compartment model with allometric scaling in which Bayesian methods were used to place uninformative priors on Cl and Vc, but informative priors based upon the full PK model on the remaining parameters in the PK model. The medians and 95% CI for Cl and Vc were obtained per the posterior distributions, and power was calculated as the proportion of replicates with a 95% CI that did not fall outside of the reference range (60–140% of the estimated typical value).

Evaluation of poor metabolizers versus extensive metabolizers

Ulotaront is metabolized in vitro in part by CYP2D6. To investigate the degree to which CYP2D6 metabolizer status affects PK, the empirical Bayes estimates (EBEs) of CL/F resulting from the full model were examined by metabolizer status. A large decrease in the CL/F in the poor metabolizer (PM) group as compared to the extensive metabolizers (EMs) would indicate a high fraction of metabolization due to CYP2D6.

RESULTS

Model development results

One and two-compartment PopPK models with first-order absorption were used to describe the plasma ulotaront concentration data. Other absorption models, such as addition of absorption lag and zero-first-order absorption, were evaluated. Ultimately, the two-compartment first-order absorption model provided the best fit to the data. The PK parameter estimates (95% CI) for the full model on the complete analysis set were: CL/F = 32.5 (28.9, 36.5) L/h; Vc/F = 232 (223, 241) L; Q/F = 0.790 (0.651, 0.959) L/h; apparent peripheral volume of distribution after oral dosing (Vp/F) = 19.3 (16.3, 22.9) L; ka = 0.966 (0.878, 1.06) h^{-1}. Interindividual variability (IIV) was included on all parameters (CL/F), apparent central volume of distribution after oral dosing (V_c/F), apparent (oral) intercompartmental clearance (Q/F), apparent peripheral volume of distribution after oral dosing (V_p/F), and absorption rate constant (k_a). Residual variability was estimated with both proportional error models alone and combined proportional and additive error models: proportional error alone gave the best fit, per AIC and Bayesian Information Criteria (BIC). Examination of the residuals by study indicates larger residual variability in phase II, but homogenous variability across the phase I studies, including those with higher LLQ.

An allometric relationship with fixed exponents was included in the base model to describe relationships between all clearance and volume parameters. Improvement was seen in estimating those weight effects, but fixed the allometric model is presented as the base model. Parameter estimates for the base model are provided in the online Table S2. Prior to any covariate adjustment aside from bodyweight, IIV was moderate-to-high in CL/F (45.5% coefficient of variation [CV]), V_p/F (42.8% CV), and high in k_a (95.2% CV), whereas lower in V_c/F at 16.8% CV.

Residual plots and diagnostics for the base model and its IIV parameters generally indicated that ulotaront was well-described by the base model. No clear trend in weight was apparent against the fitted PopPK parameters for CL/F, V_c/F, k_a, or V_p/F (available upon request from author G.R.G.) indicating adequacy of the allometric relationships. The PopPK parameters did not appear to differ by Asian/non-Asian categorization, sex, formulation (capsule or tablet), patients versus healthy volunteers, or over the range of ages studied (18–55 years).

In the full model, the effect of Asian race, patient status (healthy volunteer/patient), age (18–55 years), and sex on exposure were evaluated by adding these variables as covariates on CL/F. Point estimates (and 95% CI) of the covariate effects corresponded to a 0.821 (0.543, 1.10) effect of weight on the clearance parameters and a 0.610 (0.475, 0.745) effect of weight on the volume parameters. Further, there were minimal effects estimated for subjects of Asian ethnicity (0.987 [0.874, 1.12]), age (−0.154 [−0.322, 0.0147]), and for women (0.938 [0.843, 1.04]) on CL/F (Table 1). As seen in the base model, diagnostic plots for the full model indicated good characterization of ulotaront (see the online Supplementary section Figures S12, S13, S14, S15, S16).

TABLE 1 Pharmacokinetic parameters table for the full model

Parameter	Estimate	95% CI	%CV or ρ
CL/F (L/h)	32.5	(28.9, 36.5)	
V_c/F (L)	232	(223, 241)	
Q/F (L/h)	0.790	(0.651, 0.959)	
V_p/F (L)	19.3	(16.3, 22.9)	
k_a (1/h)	0.966	(0.878, 1.06)	
Weight_{CL}	0.821	(0.543, 1.10)	
Weight_{V}	0.610	(0.475, 0.745)	
Patient_{CL}	0.809	(0.720, 0.908)	
Asian_{CL}	0.987	(0.874, 1.12)	
Female_{CL}	0.938	(0.843, 1.04)	
Age_{CL}	−0.154	(−0.322, 0.0147)	
CL/F	0.151	(0.0801, 0.222)	40.4 (%CV)
CL/F - V_c/F	0.0379	(0.00726, 0.0685)	0.713 (ρ)
CL/F - k_a	−0.0646	(−0.213, 0.0834)	−0.248 (ρ)
CL/F - V_p/F	−0.00568	(−0.0545, 0.0431)	−0.0372 (ρ)
V_c/F	0.0187	(0.00661, 0.0308)	13.7 (%CV)
V_c/F - k_a	−0.0146	(−0.0550, 0.0257)	−0.159 (ρ)
V_c/F - V_p/F	0.0255	(0.00560, 0.0454)	0.474 (ρ)
k_a	0.450	(0.214, 0.686)	75.4 (%CV)
k_a - V_p/F	0.0573	(−0.0138, 0.128)	0.217 (ρ)
V_p/F	0.155	(0.113, 0.197)	40.9 (%CV)
Residual (proportional)	0.104	(0.0867, 0.121)	

The full model includes weight, patient status, Asian/non-Asian, and gender as covariates on relative clearance (CL/F) as well as weight as a covariate on central volume (V_c/F). Interindividual variability (IIV) was modeled on relative clearance, central volume, the absorption rate constant (k_a), and peripheral volume (V_p/F). In addition to the parameter estimates with 95% confidence intervals (CIs), also shown are percent coefficient of variation (%CV) for each parameter, and correlations (ρ) between each pair of parameters.

Model evaluation results

Five hundred Monte Carlo simulation replicates of the original data set were generated using the full PopPK model. VPCs for the studies in which PKs were sampled intensively are shown in Figure 1 (other studies are available per request). Distributions of area under the concentration versus time curve from time =0 to the time of the last quantifiable observation (AUC_{last}) and C_{max} for the simulated data were compared with the distributions of the same characteristics in the observed data sets graphically (see the Figures S17–S29). These predictive checks showed that the central location (i.e., median) of the simulations generally aligned with the observed summary-level PK metrics thought to be most relevant to downstream clinical end points. In conjunction with the VPCs, the full model was deemed suitable for purpose of simulation.

Model-based inference

Typical-value profiles over 10 days of ulotaront exposure to 7 days of q.d. dosing are shown in Figure S30. The geometric mean and SD of ulotaront plasma concentration of the 1000 resampled patients with schizophrenia reached steady-state rapidly, around the third dose, and generally cleared after 48 h. $AUC_{0\text{-}24}$, C_{trough}, and C_{max} are shown for each dose at days 1 and 3 in Table 2. In the suspected therapeutic range (e.g., 75 mg q.d.) the following increases are

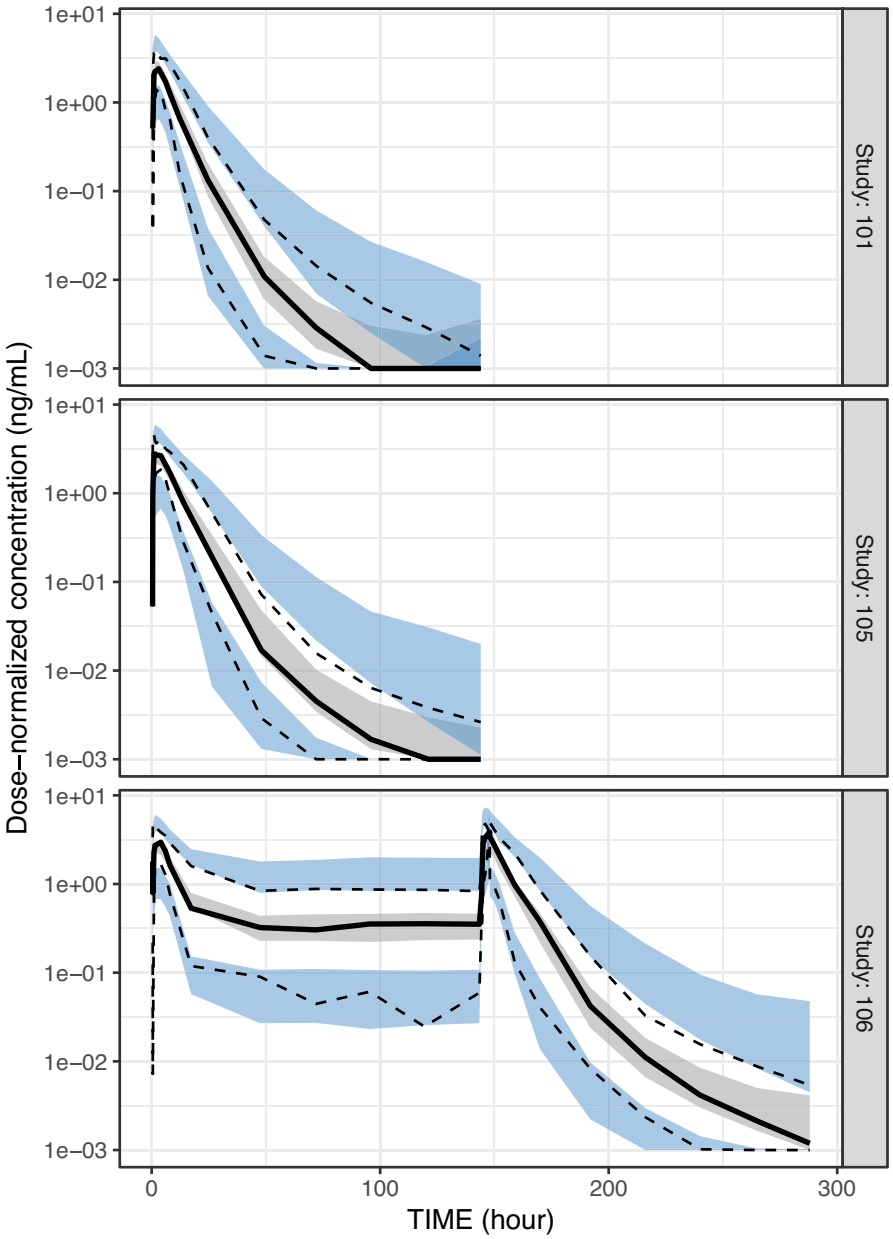

FIGURE 1 Dose-normalized visual predictive checks for ulotaront studies SEP361-101 (single ascending dose, healthy volunteers), SEP361-105 (single ascending dose, patients), and SEP361-106 (multiple dose, patients). Lines represent the observed 5th, 50th, and 95th percentiles and shaded regions represent the simulated 95% confidence intervals around each

TABLE 2 Geometric mean values for AUC_{last}, C_{trough}, and C_{max} at days 1 and 3 of multiple dosing

	Dose					
Parameter	**25 mg**	**50 mg**	**75 mg**	**100 mg**	**125 mg**	**150 mg**
Day 1						
AUC_{last}, ng/ml*h	778	1580	2410	3100	4000	4690
C_{trough}, ng/ml	7.03	14.5	22.8	27.8	37.5	42.2
C_{max}, ng/ml	69.9	142	213	280	355	424
Day 3						
AUC_{last}, ng/mL*h	866	1770	2700	3460	4490	5230
C_{trough}, ng/ml	7.97	16.5	26.0	31.5	42.8	47.9
C_{max}, ng/ml	77.7	158	238	312	398	471

This table provides the results of simulated profiles of 1000 patients with schizophrenia that were generated from the full model at 25, 50, 75, 100, 125, and 150 mg q.d. and their geometric means calculated at each time point. Using these longitudinal series of geometric means, the first and third day of AUC_{last}, C_{trough}, and C_{max} were calculated.

Abbreviations: AUC_{last}, area under the concentration-time curve from zero (predose) through the end of observation; C_{max}, maximum serum concentration; C_{trough}, minimum concentration in the dosing interval.

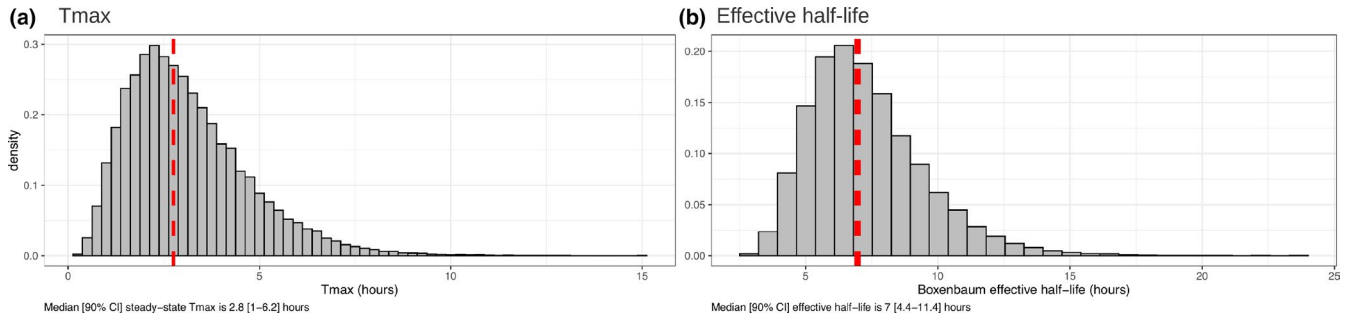

FIGURE 2 (a) Simulated ulotaront time to maximum concentration (T_{max}) after steady-state dosing of 50 mg q.d. Ten thousand (10,000) simulations were performed with resampled schizophrenia patients at steady-state: the histogram is the density of T_{max} per re-sampled patient, and the dashed red line is the median (2.8 h). (b) Simulated ulotaront effective half-life after steady-state dosing of 50 mg q.d. Ten thousand (10,000) simulations were performed with re-sampled schizophrenia patients at steady-state: the histogram is the density of the effective half-life per re-sampled patient, and the dashed red line is the median (7 h)

seen from day 1 to day 3: AUC_{0-24} increases from 2410 ng/ml*h to 2700 ng/ml*h, C_{trough} increases from 22.8 ng/ml to 26.0 ng/ml, and C_{max} increases from 213 ng/ml to 238 ng/ml. The C_{max} at day 3 increases from 78 ng/ml at 25 mg q.d. up to 471 ng/ml at 150 ng/ml.

The full model was used to evaluate the extent of influence of covariates on AUC_{ss}: weight had the greatest impact on relative AUC_{ss} with effects at the lowest and highest values that exceeded the 80–125 comparability interval (see Figure S31).

Estimates of CL/*F*, related covariate effects, and IIV in CL/*F* from the full model were used to predict exposure in Asian patients at four dose levels, relative to exposure in non-Asian patients. Though the 90% prediction intervals of exposure overlapped extensively across doses and patient populations, median values were greater in Asian patients, as compared to non-Asian patients at identical doses (see the online Figure S32). The differences can be attributed primarily to lower CL/*F* in Asian patients due to lower body weight (mean = 64.8 kg) as compared to non-Asian patients (mean = 78.8 kg).

CL/*F*, related covariate effects, and IIV in CL/*F* from the full model were used to predict exposure in healthy volunteers and patients with schizophrenia (Figure 1). The 90% prediction intervals of exposure overlap extensively across doses and subject/patient populations. Summaries of the derived metrics T_{max} (calculated at steady-state dosing), effective $t_{1/2}$, and the accumulation ratio. Figure 2a,b show the distribution of these simulations with a median (and 90% CI) T_{max} of 2.8 h (1, 6.2 h) and a median effective $t_{1/2}$ of 7 h (4.4, 11.4 h). These values correspond to an accumulation ratio (90% CI) of 1.10 (1.02, 1.30).

The distribution of the individual PK parameter random effects (i.e., η_i) across the maximal dose received in the trial setting for all phase 1a patients in the analysis population was examined for trends in

the dose-η relationship that might indicate violation of dose proportionality. No trend was apparent in CL/F, but doses 75–125 mg showed possible violations in V_c/F (i.e., the mean for those doses is not centered around 0; Figure 3a). For AUC_{0-24}, the line of proportionality fell within the 95% CIs for all doses and there was therefore no evidence of violation of dose proportionality. For C_{max}, the 95% CI for the 125 mg dose was sub-proportional but all other doses above and below covered the line of proportionality (Figure 3b and 3c). Therefore, the PKs of ulotaront is linear across the therapeutic dose range of 25–100 mg q.d.

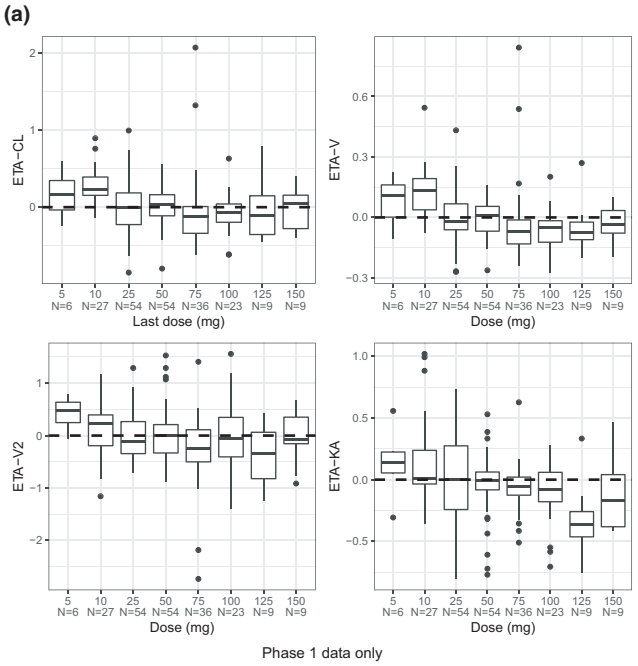

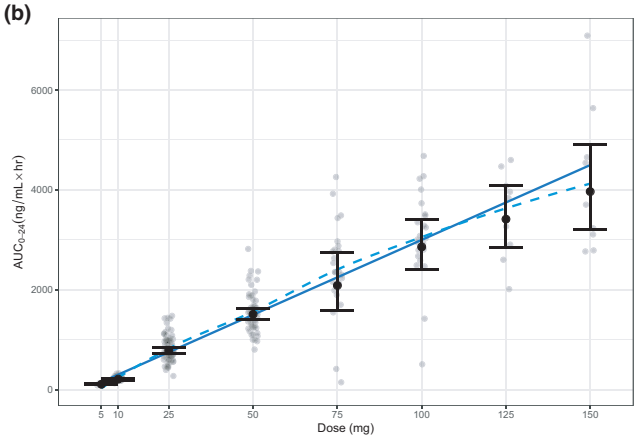

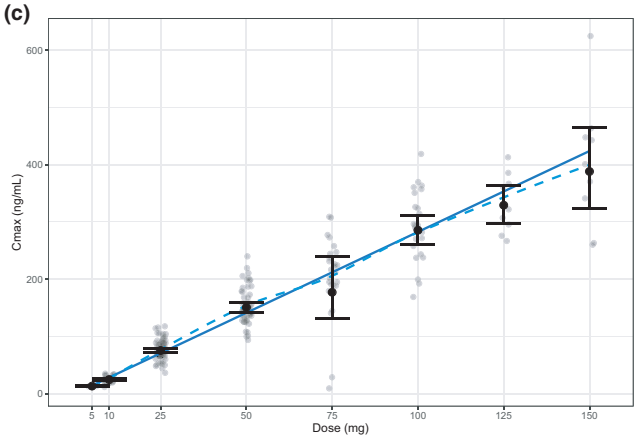

Applications of modeling and simulation

Phase III blood sampling scheme for adequate PK characterization

Simulations showed that the proposed sampling scheme would allow for adequately characterization of CL/F, but not Vc/F. Figure 4 shows the power curve for both CL/F and Vc/F as a single sample is added after the first dose for each adolescent patient, with the power dropping under the desired 80% criteria after 8 h postdose. A histogram demonstrating the observed postdose sample times in clinical trials is shown as a frame a reference for realistic postdose AM sampling times with the majority of the times corresponding to samples that do not adequately inform Vc/F. As a result of this, a single 2-h postdose sample was added to the sampling scheme in order to adequately characterize Vc/F in adolescent patients in the pivotal clinical trial.

PM versus EM comparison

Figure 5 shows a box-and-whisker plot comparing EBEs for CL/F for those patients phenotyped as PM, EM, or intermediate metabolizer (IM) CYP2D6. Despite a small number of PMs included in the studies, those that were recorded show considerable overlap with the IM and EM

FIGURE 3 (a) Estimated interindividual random effects (etas) for subjects in the phase I studies, by last dose received. (b) Observed dosing was used to simulate patient profiles on intensive sampling days (i.e., in phase I). The geometric means and their 95% confidence intervals (CIs) were calculated and compared to dose proportionality, as presented by a linear fit through the origin and all model-predicted 0–24-hour area under the concentration-time curve (AUC_{0-24}) values. The solid blue line represents the line of dose proportionality whereas the dashed line indicates a loess smooth through the model-predicted AUC_{0-24} values. (c) Observed dosing was used to simulate patient profiles on intensive sampling days (i.e., in phase I). The geometric means and their 95% CIs were calculated and compared to dose proportionality, as presented by a linear fit through the origin and all model-predicted maximum concentration (C_{max}) values. The solid blue line represents the line of dose proportionality, whereas the dashed line indicates a loess smooth through the model predicted AUC_{0-24} values

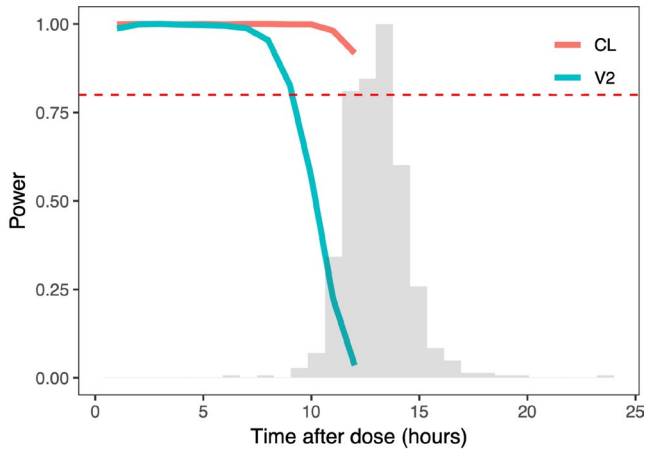

FIGURE 4 Power to estimate apparent clearance after oral dosing (CL/F) and central volume of distribution after oral dosing (Vc/F) given the proposed sampling scheme plus one single post-first-dose sample was simulated. The study was considered adequately powered if the estimated pharmacokinetic (PK) parameters fell within 60–140% of the "truth," CL/F and Vc/F from the full PK model. Power curves for each of CL/F and Vc/F are shown as the red and blue solid lines, respectively. The dashed red line represents the power criteria of 80%, and the histogram is that of all postdose AM samples in phase II (i.e., typical AM sampling times)

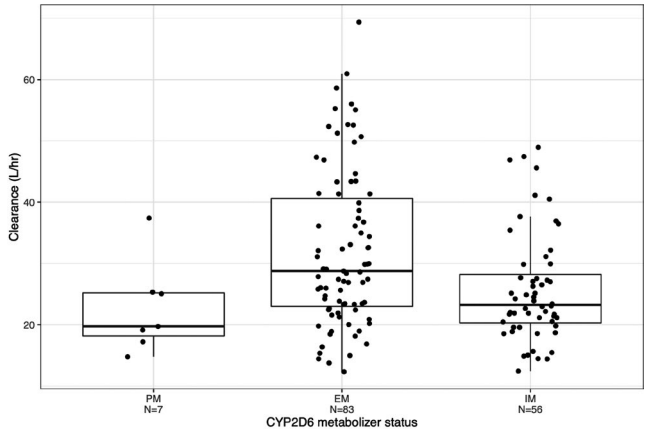

FIGURE 5 Box-and-whisker plot of the empirical Bayes estimates (EBEs) of apparent clearance after oral dosing (CL/F) by CYP2D6 metabolizer status. Points represent the EBEs, the boxes represent the 25th, 50th, and 75th percentiles of CL/F within group, and the whiskers represent 1.5 times the interquartile range (IQR). EM, extensive metabolizer; IM, intermediate metabolizer; PM, poor metabolizer

subjects indicating the CYP2D6 component of the metabolic pathway is relatively minor.

DISCUSSION

Analyses of data pooled across eight studies demonstrated that ulotaront PKs was adequately described by a two-compartment model with first-order absorption. The PK parameter estimates (95% CI) for the full model on the complete analysis set were: CL/F = 32.5 (28.9, 36.5) L/h; Vc/F = 232 (223, 241) L; Q/F = 0.790 (0.651, 0.959) L/h; apparent peripheral volume of distribution after oral dosing (Vp/F) = 19.3 (16.3, 22.9) L; ka = 0.966 (0.878, 1.06) h^{-1}. Diagnostic plots indicate that ulotaront is well-described by the base model.

To avoid well-documented problems associated with stepwise regression techniques in their handling of correlated or collinear predictors, treatment of multiple comparisons, artificially optimistic parameter precision, and a lack of biologic rationale for significant predictors, a covariate modeling approach emphasizing parameter estimation rather than stepwise hypothesis testing was implemented for this analysis. The only meaningful covariate affecting PK parameters was body weight. After accounting for body weight, no clinically relevant impact on PK parameters was observed for the following covariates: clinical status (healthy volunteer vs. patient with schizophrenia), race (non-Asian vs. Asian, predominately Japanese), sex, and age (18–55 years). This population model incorporates several different populations (e.g., patients and healthy volunteers, different treatment histories, different regions, but a broad range of weights). We note that covariate effects are sensitive to both the studied covariates and any confounders of those covariates, which is why emphasis was placed upon evaluation of clinical relevance through simulation.

Overall, ulotaront showed a PK profile that supported q.d. dose administration. Absorption of ulotaront occurred quickly with a median T_{max} of 2.8 h. Ulotaront cleared quickly from plasma with a median effective $t_{1/2}$ of 7 h, leading to an accumulation ratio of 1.1 upon daily dosing to steady-state. Linear PK dose-proportionality was evident for ulotaront at therapeutic dose levels ranging from 25 mg to 100 mg q.d.

The full model has been used to simulate outcomes and define optimal dose regimens and blood sampling schemes to characterize the PK of ulotaront in adolescent patients with schizophrenia (13 to 17 years), subjects with organ impairment, drug-interaction studies, and other clinical pharmacology studies. Further, the population PK data are being combined with pharmacodynamic results to characterize the therapeutic window for ulotaront and to establish optimal dose regimens in subpopulations.

ACKNOWLEDGEMENTS

Sunovion discovered Ulotaront in collaboration with PsychoGenics based in part on a mechanism-independent approach using the in vivo phenotypic SmartCube platform and associated artificial intelligence algorithms.

CONFLICTS OF INTEREST

G.R.G., S.C.H., and K.S.K. are employees of Sunovion Pharmaceuticals, Inc. D.G.P. and J.M.F. are employees of Metrum Research Group and were working under a contract from Sunovion Pharmaceuticals, Inc.

AUTHOR CONTRIBUTIONS

G.R.G. and D.G.P. wrote the manuscript. G.R.G., S.C.H., and K.S.K. designed the research. G.R.G., D.G.P., and J.M.F. performed the research. G.R.G., D.G.P., J.M.F., and S.C.H. analyzed the data. K.S.K. and S.C.H. contributed to new reagents.

REFERENCES

1. Lieberman JA, Stroup TS, McEvoy JP, et al. Effectiveness of antipsychotic drugs in patients with chronic schizophrenia. *N Engl J Med*. 2005;353(12):1209-1223.
2. Leucht S, Cipriani A, Spineli L, et al. Comparative efficacy and tolerability of 15 antipsychotic drugs in schizophrenia: a multiple-treatments meta-analysis. *Lancet*. 2013;382(9896):951-962.
3. Laursen TM, Nordentoft M, Mortensen PB. Excess early mortality in schizophrenia. *Annu Rev Clin Psychol*. 2014;10:425-448.
4. Cooper SJ, Reynolds GP, Barnes T, et al. BAP guidelines on the management of weight gain, metabolic disturbances and cardiovascular risk associated with psychosis and antipsychotic drug treatment. *J Psychopharmacol*. 2016;30:717-748.
5. Taipale H, Mittendorfer-Rutz E, Alexanderson K, et al. Antipsychotics and mortality in a nationwide cohort of 29,823 patients with schizophrenia. *Schizophr Res*. 2017;S0920–9964(17):30762-30764.
6. Stahl SM, Buckley PF. Negative symptoms of schizophrenia: a problem that will not go away. *Acta Psychiatr Scand*. 2007;115:4-11.
7. Krause M, Zhu Y, Huhn M, et al. Antipsychotic drugs for patients with schizophrenia and predominant or prominent negative symptoms: a systematic review and meta-analysis. *Eur Arch Psychiatry Clin Neurosci*. 2018;268:625-639.
8. Revel FG, Moreau JL, Gainetdinov RR, et al. TAAR1 activation modulates monoaminergic neurotransmission, preventing hyperdopaminergic and hypoglutamatergic activity. *Proc Natl Acad Sci*. 2011;108:8485-8490.
9. Lindemann L, Meyer CA, Jeanneau K, et al. Trace amine-associated receptor 1 modulates dopaminergic activity. *J Pharmacol Exp Ther*. 2008;324:948-956.
10. Rutigliano G, Accorroni A, Zucchi R. The case for TAAR1 as a modulator of central nervous system function. *Front Pharmacol*. 2018;8:987.
11. Gainetdinov RR, Hoener MC, Berry MD. Trace amines and their receptors. *Pharmacol Rev*. 2018;70:549-620.
12. Pei Y, Asif-Malik A, Canales JJ. Trace amines and the trace amine-associated receptor 1: pharmacology, neurochemistry, and clinical implications. *Front Neurosci*. 2016;10:48.
13. Schwartz MD, Canales JJ, Zucchi R, et al. Trace amine-associated receptor 1: a multimodal therapeutic target for neuropsychiatric diseases. *Expert Opin Ther Targets*. 2018;22:513-526.
14. Wolinsky TD, Swanson CJ, Smith KE, et al. The trace amine 1 receptor knockout mouse: an animal model with relevance to schizophrenia. *Genes Brain Behav*. 2007;6:628-639.
15. Leo D, Mus L, Espinoza S, et al. Taar1-mediated modulation of presynaptic dopaminergic neurotransmission: role of D2 dopamine autoreceptors. *Neuropharmacology*. 2014;81:283-291.
16. Dedic N, Jones PG, Hopkins SC, et al. SEP-363856, a novel psychotropic agent with a unique, non-D2 receptor mechanism of action. *J Pharmacol Exp Ther*. 2019;371:1-14.
17. Hopkins SC, Dedic N, Koblan KS. Effect of TAAR1/5-HT_{1A} agonist SEP-363856 on REM sleep in humans. *Transl Psychiatry*. 2021;11:228.
18. Kokkinou M, Irvine EE, Bonsall DR, et al. Reproducing the dopamine pathophysiology of schizophrenia and approaches to ameliorate it: a translational imaging study with ketamine. *Mol Psychiatry*. https://doi.org/10.1038/s41380-020-0740-6.
19. Koblan KS, Kent J, Hopkins SC, et al. A non–D2-receptor-binding drug for the treatment of schizophrenia. *N Engl J Med*. 2020;382:1497-1506.
20. Soldin OP, Mattison DR. Sex differences in pharmacokinetics and pharmacodynamics. *Clin Pharmacokinet*. 2009;48:143-157.
21. Kim K, Johnson JA, Derendorf H. Differences in drug pharmacokinetics between East Asians and Caucasians and the role of genetic polymorphisms. *J Clin Pharmacol*. 2004;44:1083-1105.
22. American Psychiatric Association. *Diagnostic and Statistical Manual of Mental Disorders*, 4th ed., Text Revision. Washington, DC: American Psychiatric Association, 2000.
23. American Psychiatric Association. *Diagnostic and Statistical Manual of Mental Disorders*, 5th edn. Washington, DC: American Psychiatric Association; 2013.
24. Guy W. *ECDEU Assessment Manual for Psychopharmacology—Revised (DHEW Public No ADM76-338) 534-537*. Rockville, MD: U.S. Department of Health, Education, and Welfare; Public Health Service, Alcohol, Drug Abuse, and Mental Health Administration, NIMH Psychopharmacology Research Branch, Division of Extramural Research Programs; 1976.
25. Kay S, Fiszbein A, Opler L. The positive and negative syndrome scale (PANSS) for schizophrenia. *Schizophr Bull*. 1987;13:261-276.
26. Gastonguay MR. A full model estimation approach for covariate effects: inference based on clinical importance and estimation precision. *AAPS Journal*. 2004;6(S1):Abstract W4354.
27. Burnham KP, Anderson DR. *Model Selection and Multimodel Inference: A Practical Information-Theoretic Approach*. New York: Springer-Verlag; 2002.
28. Boxenbaum H, Battle M. Effective half-life in clinical pharmacology. *J Clin Pharmacol*. 1995;35(8):763-766.
29. Wang Y, Jadhav PR, Lala M, et al. Clarification on precision criteria to derive sample size when designing pediatric pharmacokinetic studies. *J Clin Pharmacol*. 2012;52(10):1601-1606.
30. National Health and Nutrition Examination Survey (NHANES). http://www.cdc.gov/nchs/nhanes/. Accessed August 30, 2018.

SUPPORTING INFORMATION

Additional supporting information may be found online in the Supporting Information section.

How to cite this article: Galluppi GR, Polhamus DG, Fisher JM, Hopkins SC, Koblan KS. Population pharmacokinetic analysis of ulotaront in subjects with schizophrenia. *CPT Pharmacometrics Syst Pharmacol*. 2021;10:1245–1254. https://doi.org/10.1002/psp4.12692